Preliminary study of HCHO spatial and temporal distribution from Coastal to Plateau areas in Antarctica

Ombretta Largiuni[a]; Emiliano Castellano[a]; Alessio Migliori[a]; Rita Traversi[a]; Giovanni Piccardi[a]; Roberto Udisti[a]

[a] Department of Chemistry, University of Florence, Via della Lastruccia 5, I-50121 Sesto Fiorentino, Italy

PLEASE SCROLL DOWN FOR ARTICLE

Taylor & Francis
Taylor & Francis Group

PRELIMINARY STUDY OF HCHO SPATIAL AND TEMPORAL DISTRIBUTION FROM COASTAL TO PLATEAU AREAS IN ANTARCTICA

OMBRETTA LARGIUNI*, EMILIANO CASTELLANO, ALESSIO MIGLIORI,
RITA TRAVERSI, GIOVANNI PICCARDI and ROBERTO UDISTI

*Department of Chemistry, University of Florence,
Via della Lastruccia 5, I-50121 Sesto Fiorentino, Italy*

Formaldehyde concentrations were determined in over 1800 snow samples (snowpit, firn cores and superficial snow) from Antarctica by a sensitive spectrofluorimetric Flow Injection Analysis method. The method performances (detection limit: 55 ng/L; reproducibility: 2.5% at 1 μg/L level; linear range: 0.1–3000 μg/L) allowed a reliable determination of formaldehyde content in all the collected samples. The range of determined concentrations was 0–70 μg/L with a mean concentration of 7.7 μg/L and a median concentration of 5.8 μg/L. The formaldehyde background level was estimated at a few micrograms per liter in coastal and plateau areas of Northern Victoria Land. In some stations the background values are modulated by HCHO deposition events recurring over relatively large time periods.

Keywords: Formaldehyde; Flow analysis; Antarctica; Snow

INTRODUCTION

Formaldehyde is involved in oxidative processes of anthropic and natural carbon cycle compounds in the atmosphere. It is both emitted directly into the atmosphere (from combustion processes and from biogenic sources) and produced *in situ* during the photodegradation of organic compound (e.g., anthropic and biogenic hydrocarbons) [1–3].

In anthropic environments, where marked concentrations are measured, the study of the spatial and temporal distribution of formaldehyde is important to assess the effects of this pollutant on the environment, because it is toxic for animal and plant life. In particular, formaldehyde is receiving attention because of its carcinogenic effect [4].

Formaldehyde depositions are also recorded in polar ice sheets, where it is carried by long-range transport of carbonyl compounds and their precursors; *in situ* sources originate from marine biogenic emissions by algal and microbial metabolic processes

---

*Corresponding author. Fax: +39-55-4579985. E-mail: ombretta.largiuni@unifi.it

and from photolysis of organic matter coming from the free sea surface and from the organisms enclosed in the pack ice [5].

Formaldehyde measurements can give information on the variations in biogeochemical cycles on regional and global scales, closely correlated to the climatic changes. Formaldehyde is a key reactive intermediate in the hydrocarbon oxidation chain; in the remote troposphere CH_4 is the dominant formaldehyde precursor and thus information on formaldehyde seems to be useful in understanding the methane oxidation process. In the remote marine boundary layer the contribution of non-methane volatile organic carbon (NMVOC) oxidation to the formaldehyde budget can amount to around 20%; in particular isoprene oxidation can provide a significant formaldehyde source. A further unknown in the formaldehyde budget is the effect of halogen chemistry; e.g., the reactivity of Cl atoms is high enough to abstract hydrogen atoms from CH_4 and thus increase the formaldehyde concentration by an enhanced CH_4 oxidation rate [6].

Formaldehyde plays a role in the oxidizing capacity of the troposphere because of its interactions with H_2O_2 and with OH and HO_2 radicals. Formaldehyde itself acts as an important free radical precursor (by photolysis reactions) and its contribution can be compared to that of O_3 [7]. Formaldehyde archived in the polar ices, mainly produced in the atmosphere by radical reactions closely linked to the OH radical content, potentially allows the setting up of models for a reliable estimation of OH radical concentration changes in the past and reconstruction of the oxidative capacity of the paleo-atmospheres [8]. However, there is still a lack of information about mechanisms of formaldehyde deposition, post-depositional air–snow exchange, possible chemical reactions in buried snow and firn and of the atmospheric chemistry of formaldehyde in polar regions [9].

The Antarctic region is of great interest in environmental studies, because is located far from other continents and thus provide the cleanest atmospheric environment. Few formaldehyde data in Antarctic ice sheet have been reported until now and such measurements are mainly related to studies of the temporal profile of this compound in different climatic periods [10–12]. To overcome the information gap on the spatial distribution of formaldehyde in fresh and recent (over the last 50 years) Antarctic snow depositions, several samples, collected in coastal and plateau areas, were analysed. Some preliminary results are reported here.

Because of its low concentration levels (a few parts per billion) in snow and ice and of contamination problems by uptake from laboratory air, formaldehyde determination was performed by a sensitive spectro-fluorimetric flow injection analysis (SF-FIA) method, able to limit, as much as possible, any sample manipulation and contact with the laboratory environment. The method is based on the reaction of formaldehyde with acetylacetone, acetic acid and ammonium ions to form diacetyldihydrolutidine, a fluorescent compound [13]. The addition of a non-ionic surfactant decreases the fluorescence quenching, increasing the signal/noise ratio [14].

Improvements in the method have made possible the determination of formaldehyde in Antarctic snow and firn samples even where present at concentrations lower than $1 \mu g/L$

Formaldehyde content was determined in snowpit, firn cores and superficial snow samples collected in coastal and plateau areas of Northern Victoria Land (Antarctica) to evaluate the spatial and temporal variability of this compound and trends with altitude and distance from the sea.

EXPERIMENTAL

Materials and Methods

Formaldehyde determination was performed using a spectro-fluorimetric method based on the formation of a fluorescent compound (diacetyldihydrolutidine) by the Hantzsch reaction between formaldehyde and acetylacetone, acetic acid and ammonium acetate. A surfactant (triton X-100) was used to decrease the quenching effects, increasing the fluorescence signal.

Measurements were made using a Shimadzu RF-551 spectrofluorimeter; the excitation and emission wavelengths were respectively $\lambda_{ex} = 410$ nm and $\lambda_{em} = 502$ nm.

A FIA apparatus allowed the injection of 250 μL of sample into a flux of 1.09 mL/min of UHQ water, used as carrier. A flux of 0.19 mL/min of the reagent solution (acetic acid 0.177 M, acetylacetone 0.145 M and ammonium acetate 2 M) was subsequently added and the reaction coil (0.5-mm internal diameter, 200 cm long) was warmed to 70°C. After the reaction, 0.19 mL/min of triton X-100 at 10% w/w was added to protect the fluorescence. Data acquisition and elaboration were performed by a CSW version 1.7 Date Apex Ltd. integration program.

All solutions were prepared with Merck reagents grade chemicals and UHQ water (conductivity < 18 MΩ, obtained by a Millipore-Milli Q system and continuously recycled by an Elga UHQ apparatus).

The detection limit was 55 ng/L and the response was linear in the range 0.1–3000 μg/L; for concentration of a few micrograms per liter, the reproducibility was better than 2.5%. A detailed description of the analytical apparatus and of the method performance is reported in Largiuni et al. [14].

Sampling and Decontamination

To evaluate the formaldehyde spatial distribution in coastal areas of Northern Victoria Land and along a coast-to-plateau transect from Terra Nova Bay to Dome C (East Antarctica, Pacific/Indian Ocean sector), over 1800 snow and firn samples were analyzed. The samples were collected during several Italian Antarctic campaigns from 1993/1994 to 1997/1998 in the frameworks of PNRA (Programma Nazionale di Ricerche in Antartide) and ITASE (International Trans-Antarctic Scientific Expedition) projects. The samples was obtained by drilling firn cores (Hercules Névé and Talos Dome), from snowpits (Styx Glacier, Pilot Glacier, Prince Albert, Evans Névé and Dome C) and superficial snow collection (about 100 samples). Some of the sampled stations are related to vertical (Mt. Melbourne) and horizontal (Reeves Névé and Rennick Glacier) transects in the area of Terra Nova Bay. The location and characteristics of the sampling stations are reported in Fig. 1 and in Table I.

The firn cores were taken using a special manual corer made with a minimum of metallic material to reduce contamination risks; this corer, thoroughly cleaned before use, produced core segments 50–70 cm long, which were cleaned externally on site, classified, placed in double polyethylene sealed bags and transported frozen (at −20°C). In Italy, in a cold chamber, working under a class 100 laminar flow hood, the pieces were divided into sub-samples approximately 3 cm long and stored at −20°C in pre-cleaned polyethylene containers placed in double polyethylene bags [15].
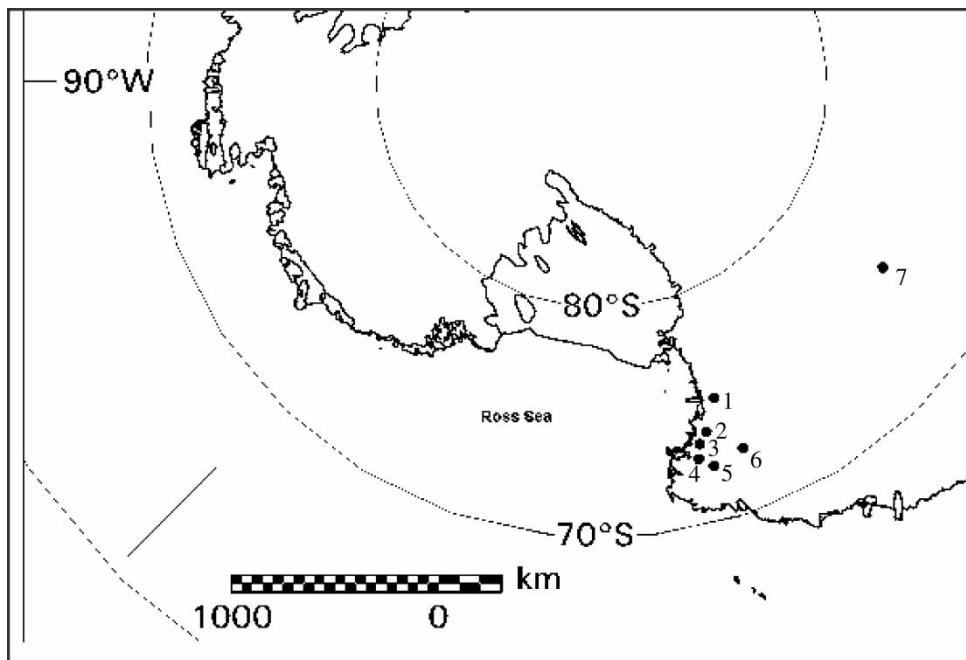
FIGURE 1   Map of Antarctica showing the sampling stations: (1) Prince Albert; (2) Styx Glacier; (3) Pilot Glacier; (4) Hercules Névé; (5) Evans Névé; (6) Talos Dome; (7) Dome C.

TABLE I   Sampling sites and their geographical characteristics

Station	Coordinates		Altitude (m a.s.l.)	Sea distance (km)	Mean snow accumulation[a] (kg m−2 yr−1)	Sample[b]
Styx Glacier	73°51.940′S	163°41.715E	1660	50	170	FS
Pilot Glacier	73°15.835′S	165°30.772′E	2100	65	200	FS
Prince Albert	75°10.300′S	162°07.530′E	800	40		FS
Evans Névé	74°42.2′S	166°56.4′E	2520	132	110	FS
Dome C	75°07′35″S	123°16′58.8″E	3309	1080	30	FS
Hercules Névé	73°06.378′S	165°27.785′E	2960	80	145	FC
Talos Dome	72°48′S	159°06′E	2340	300	86	FC
Priestley Névé	73°38′18″S	160°38′32″E	1983	145		SN
Mt. Melbourne	74°25′S	164°43′E	360–2670 vert. trans.	20		SN
Mt. Crummer	75°03.900′S	162°32.820′E	780	25		SN
Vegetation Island	74°47.326′S	163°38.439′E	100	15		SN
Snowy Point	74°35.688′S	163°49.314′E	920	5		SN
Corner Glacier	74°21.893′S	163°44.160′E	1430	25		SN
McCarthy Ridge	74°36.001′S	163°03.131′E	870	45		SN
Hercules Névé	73°06.378″S	165°27.785′E	2960	90		SN
Mt Abbott	74°42.640′S	163°52.130′E	890	5		SN
Reeves Névé	74°S	159°E	1540–2320	80–165 horiz. trans.		SN
Rennick Glacier	72°50′S	162°40′E	1350–2210	105–185 horiz. trans.		SN
Prince Albert	75°10.300′S	162°07.530′E	800	40		SN
Niggly Névé	72°42.2′S	166°30.30′E	2610	92		SN

[a]For some stations values are missing because reliable measurements are not available.
[b]FC = firn core, FS = firn snowpit, SN = superficial snow.

The snowpit samples were collected using a method developed to minimize contamination risks inserting pre-cleaned polyethylene vials (16×100 mm or 35×100 mm) directly into the snowpit walls, after having removed 10 cm of snow from the exposed surface with pre-cleaned polyethylene scoops; while working the operators wore full clean-room garb, polyethylene gloves and particle masks [16,17]. The resolution of the sampled snow layers was similar to the external diameter of the vial (16 or 35 mm).

The superficial snow was collected in pre-cleaned polyethylene containers (250 mL).

The samples, collected by different procedures, were kept at $-20°C$ and preserved until analysis. Then, while still in the same sampling containers, they were melted under a class 100 laminar flow hood and analyzed immediately after melting.

Control blanks were tested periodically for the sampling and analysis procedures and for the cleanliness of the containers, which showed contamination values below the detection limit or at least two orders of magnitude lower than the concentration values determined in the samples [18].

RESULTS AND DISCUSSION

Spatial Distribution

Figure 2 represents the descriptive statistics (box plots) of the whole data set, subdivided into coastal (up to 80 km inland), intermediate (80–200 km from the coast) and plateau (more than 300 km inland) stations.

Each box includes 50% of the data, with the median value displayed as a line. The top and bottom of box mark the limits of $\pm 25\%$ of the variable population, upper quartile (UQ) and lower quartile (LQ), so that the height of the box is the interquartile distance (i.d.). The lines extending from the top and bottom of each box include the
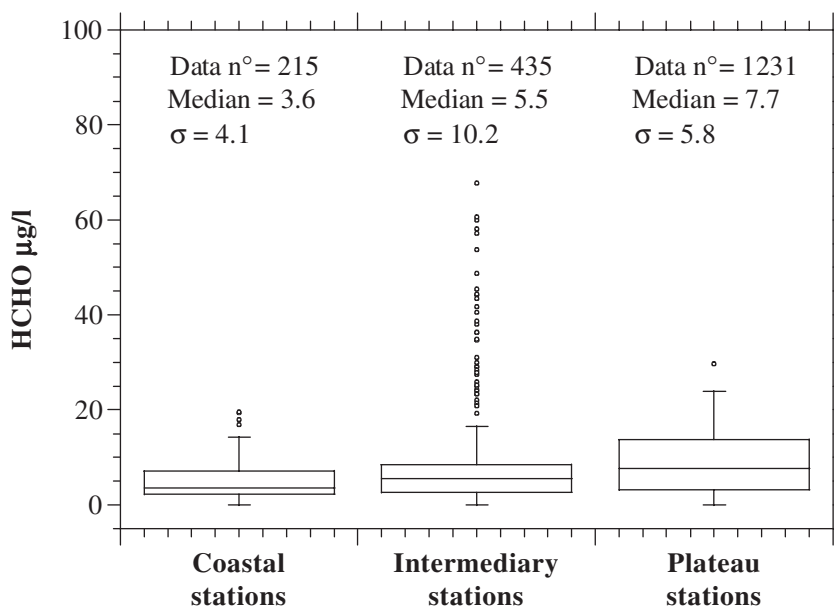

FIGURE 2   Box plots of the analyzed data whole set.

data falling within an acceptable range $[(LQ - 1.5 \times i.d.)/(UQ + 1.5 \times i.d.)]$. Any value outside this range (outlier) is displayed as an individual point.

Distribution data show similar HCHO concentration in all three station types, with a slight increase of the median value and of the data dispersion as the distance from the sea increases. Median values are around 5 ppb and 50% of the data are included in the narrow range 2–12 ppb.

The overall HCHO mean concentration is $7.7 \pm 6.8 \,\mu g/L$, in the range $0–70 \,\mu g/L$. This concentration range is larger than those obtained from Greenland ($0–24 \,\mu g/L$ [19,20]) and Antarctic ($0–25 \,\mu g/L$ [8]) ice cores, but should be noted that the data presented here are from several stations, located at very different geographic positions, such as distance from the coastal line, altitude, mean annual temperature and snow accumulation rate, so a higher data variability is to be expected. On the other hand, considering only the data enclosed inside the box plots shown in Fig. 2 (central 50% of the data distribution), the concentration range (2–12 ppb) is very close to that recently measured at Law Dome (Antarctica): $1.4–14.3 \,\mu g/L$ [10].

Table II summarizes the basic statistical information, showing also the background value (B) for each station. The background value was calculated as the mean concentration of a sub-data set obtained by excluding the samples with concentration values three times higher than the standard deviation. These values, ranging from 2.5 to $13.2 \,\mu g/L$, agree with the above reported concentration range including the central 50% of all samples, and are similar to those measured in different Antarctic areas: $0–10 \,\mu g/L$ is the concentration range encountered in the Dome C Ice Core during the Holocene period [11].

The stations where firn cores and snowpits were sampled are sorted, in Fig. 3, as the distance from the sea (and, generally, also altitude) increases, with Prince Albert the nearest to and Dome C the farthest station from the coastline. The box plots confirm the previously cited substantial uniformity of median values and data dispersion, independently of altitude and distance from the sea. Higher data dispersions are shown at the stations where a higher number of samples were analyzed (Styx Glacier, Talos Dome). An exception is found at the Evans Névé station, where a very large data dispersion is observed. We have no explanation for this, because the geographic position of the Evans Névé station (2520 m a.s.l., 130 km from the sea) provides no obvious justification for this pattern. Indeed, the very asymmetrical position of the median, located at the bottom of the box, indicates that various samples, with anomalously high HCHO concentrations, increase the mean value and the dispersion.

To distinguish the role of altitude and distance from the sea, superficial snow was collected along two transects: the first was sampled on the slopes of Mt. Melbourne,

TABLE II   Statistical parameters of the HCHO concentrations

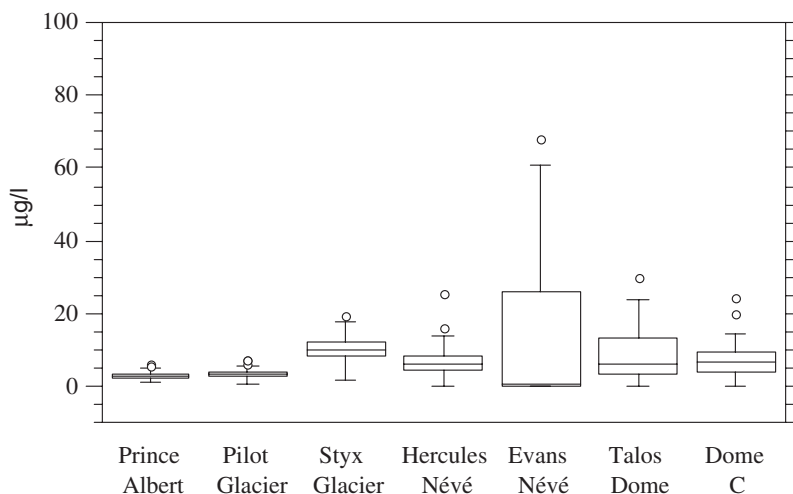| Sampling station	Number of data	Minimum (µg/L)	Maximum (µg/L)	Mean (µg/L)	Median (µg/L)	LQ (µg/L)	UQ (µg/L)	σ (µg/L)	B (µg/L)
Styx Glacier	59	1.8	19.5	10.1	9.7	8.1	12.3	3.6	8.0
Pilot Glacier	60	0.7	7.3	3.3	3.3	2.6	3.9	1.4	2.8
Prince Albert	27	1.0	6.2	2.9	2.7	2.1	3.3	1.3	2.5
Evans Névé	111	0.0	67.8	13.2	0.6	0.0	25.5	18.5	13.2
Dome C	135	0.0	24.2	6.7	6.6	4.0	9.1	3.8	6.0
Hercules Névé	288	0.2	25.2	6.3	6.0	4.2	8.1	2.9	5.4
Talos Dome	1093	0.0	29.7	7.8	5.8	3.4	13.3	5.7	7.1

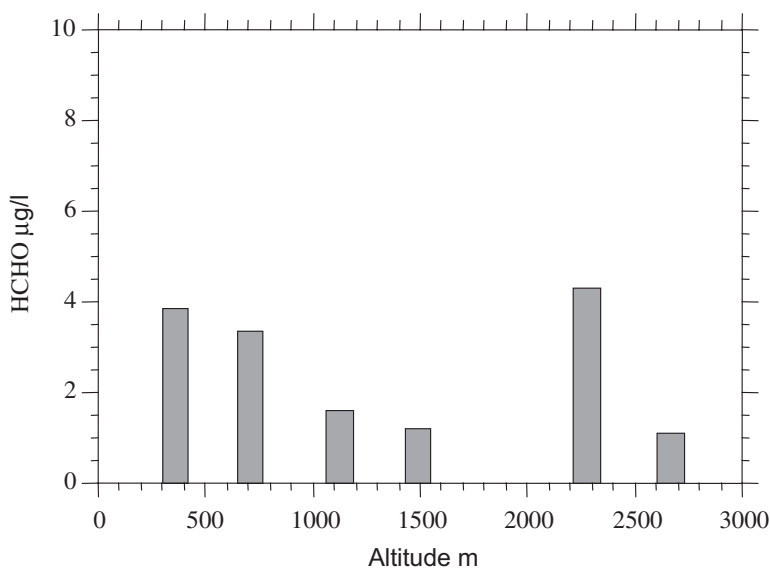FIGURE 3   Box plots for individual sampling stations.

FIGURE 4   HCHO concentration *vs*. altitude for the Mt. Melbourne vertical transect.

in the altitude range 360–2670 m a.s.l., where distance from the sea can be considered constant. Figure 4 shows a sharp reduction in HCHO concentration as altitude increases, with the exception of the site located at 2300 m a.s.l.

The second transect was sampled along the Rennick Glacier, which flows toward the Pacific Ocean behind the Transantarctic Mountains (Fig. 5). For this transect, altitude and distance from the nearest coast line (Ross Sea) vary inversely. Figure 5 shows HCHO profiles as a function of the distance from the sea (Fig. 5a) and of the altitude (Fig. 5b).

The relationship between HCHO concentration and altitude confirms the Melbourne observation, showing a concentration decrease as altitude increases. On the other hand,
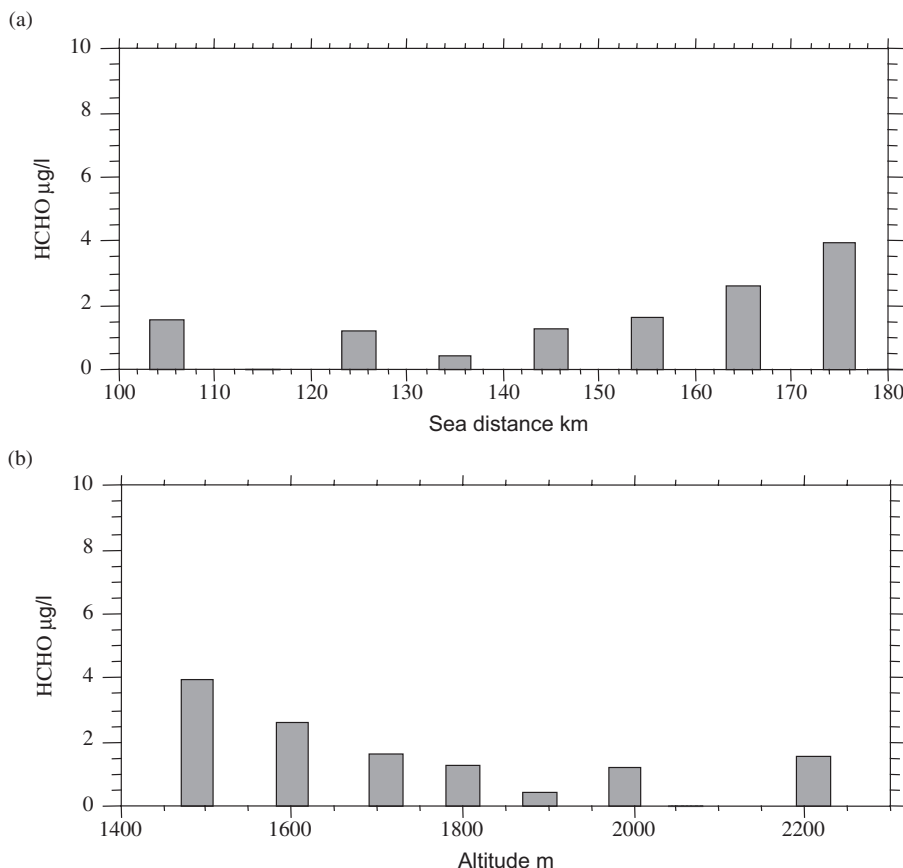
(a)

(b)

FIGURE 5   HCHO concentration *vs.* (a) sea distance and (b) altitude for the Rennick Glacier horizontal transect.

the Rennick transect confirm also the trend shown in Fig. 2, where a slight concentration increase is visible as the distance from the sea increases. As a consequence, the distance from the coast line, rather than altitude, seems to be the most crucial parameter for HCHO concentration increase in snow depositions. This pattern is probably due only to the lower dilution effect of the less frequent and intense snow precipitations in the internal areas of Antarctica, causing lower snow accumulation rates.

However, the HCHO concentration changes are very limited, often only 1–3 µg/L. Therefore, the new data set reported here supports the conclusion that the HCHO content in superficial and recent snow in coastal and plateau regions in Antarctica is spatially rather invariant, at around a few micrograms per liter, with the exception of depositions related to particular events, such as anthropic inputs or biomass burning emissions (see below)

Temporal Profiles

The HCHO concentration/depth profiles at the seven stations are shown in Fig. 6.

No particular trend is visible in any of the snowpit samples (Fig. 6a–e). The temporal periods covered by the snowpit samples range from a few years at the coastal stations to

about 45 years at Dome C, so that Antarctic precipitation does not seem to show changes in HCHO profiles for the last few tens of years. In contrast, at Talos Dome (Fig. 6g) and, with less evidence, at Hercules Névé (Fig. 6f), the firn core profiles show a more interesting trend.

At Talos Dome, two depth ranges are characterized by relatively high values: the sections 150–650 cm and 10–21 m, where HCHO concentration as high as 20–25 µg/L were measured. The two firn core sections correspond to the temporal periods 1988–1963 and 1944–1870, respectively. In the same depth ranges, other components, such as Ca, K, ammonium, fluorides and carboxylic acids, also show a sharp increase, but not the typical markers of the primary (Na^+, Cl^-) and secondary marine contributions ($nssSO_4^{2-}$, MSA) [21].
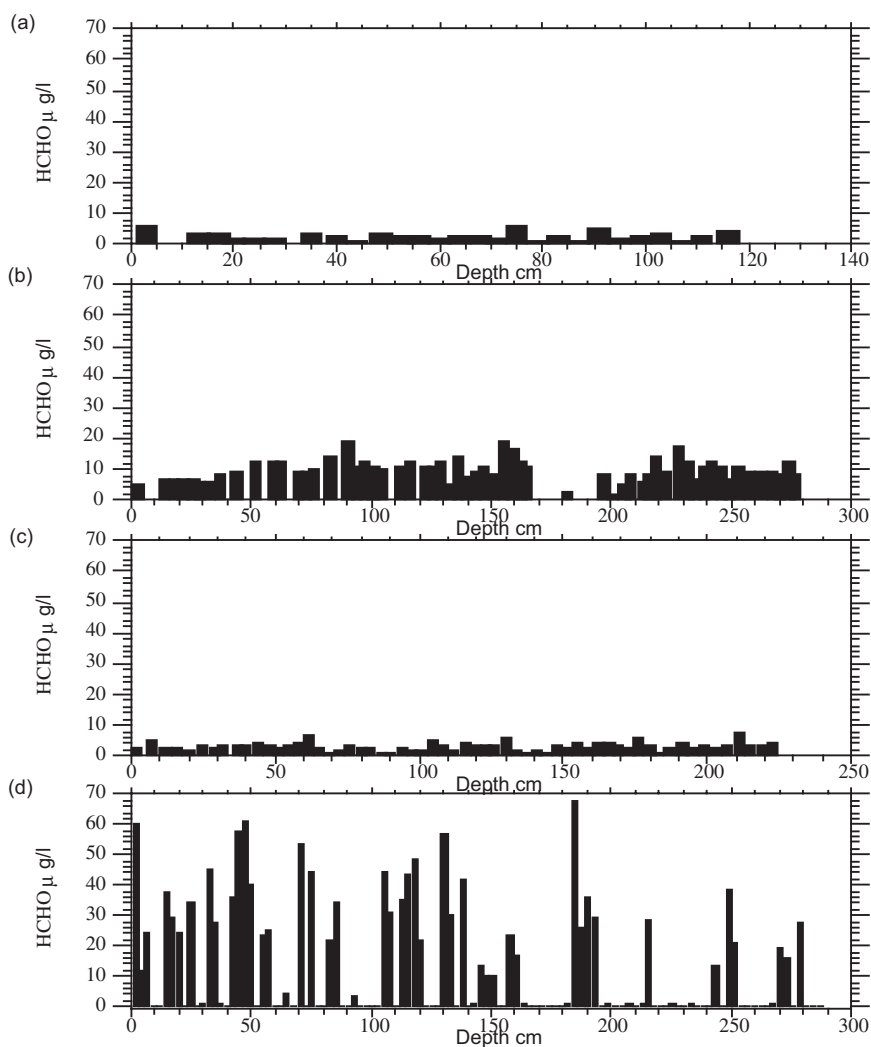

FIGURE 6 Concentration/depth profiles for (a) Prince Albert; (b) Styx Glacier; (c) Pilot Glacier; (d) Evans Névé; (e) Dome C; (f) Hercules Névé and (g) Talos Dome.
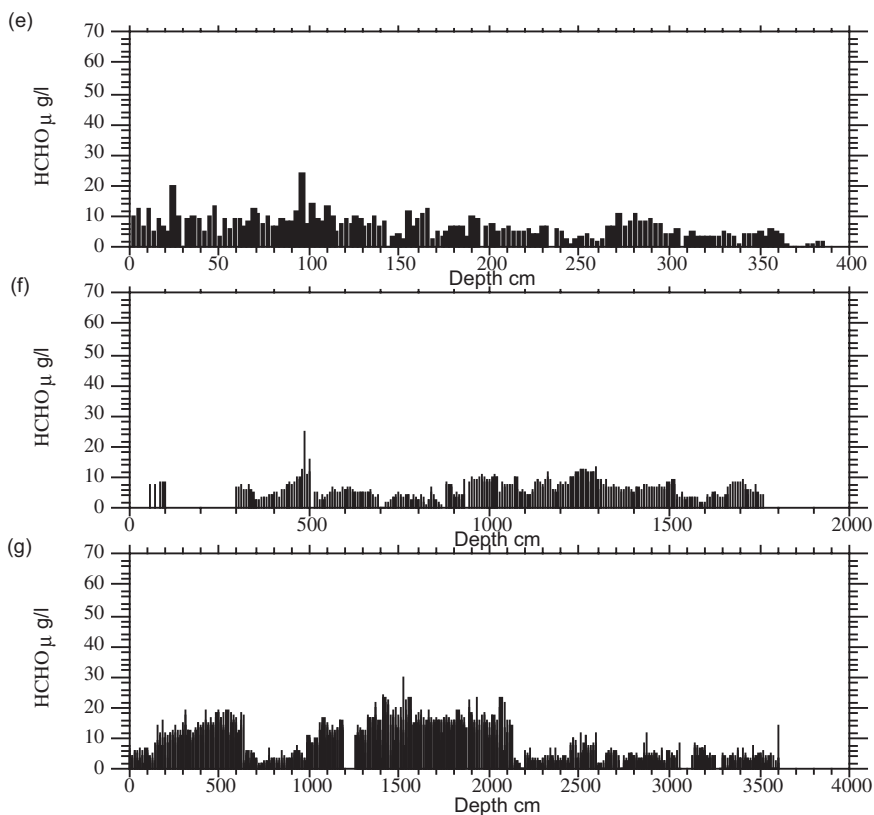
FIGURE 6   Continued.

Figure 7 shows the comparison of the HCHO trend with the Ca^{2+} and formate profiles. Sharp concentration increases are visible also for these two compounds in the same depth range. It is particularly evident for Ca, which can be used as a crustal marker. In the 10–21 m depth range, high values of $\delta^{18}O$ and dust have also been found [22], indicating a relatively warm and dry period. One hypothesis is that these climatic conditions could have encouraged desertification phenomena and caused an increase in the frequency and intensity of forest fires in the continental areas closest to Antarctica (i.e., Australia and South America), justifying the presence of high atmospheric load of dust (and high Ca^{2+} content) and short-chain organic compounds (formaldehyde and formate), that can be used as biomass burning markers.

Measurements carried out on Hercules Névé samples in the depth range 14–22 m (maximum depth reached for this firn core), corresponding to the 1947–1926 period, confirmed high concentrations of dust [23] and short-chain carboxylic acids (acetates, formates and propionates) and indicated an increase of ammonium, K and fluoride, all substances that can be correlated to emissions from biomass burning events [24]. Like Talos Dome, Hercule Névé samples do not show any increase of other components coming from different sources, such as sulphur (MSA as biogenic indicator, $nssSO_4^{2-}$ as biogenic and volcanic marker) or sea spray (Na^+ and Cl^-) compounds. For this reason, alternative sources, other than biomass burning, can probably be
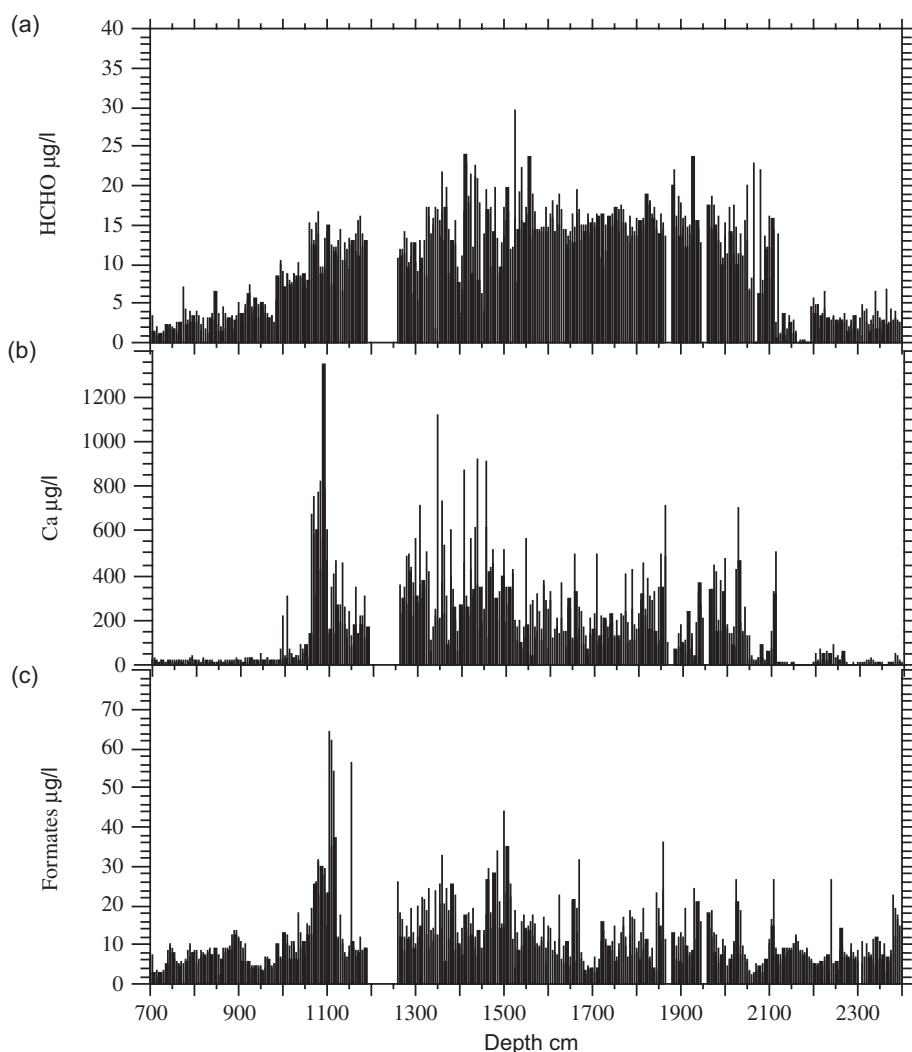
FIGURE 7 Comparison of the profiles for (a) HCHO; (b) Ca^{2+} and (c) formates in the Talos Dome firn core (10–21 m).

excluded. Moreover, preliminary analysis of insoluble particles included in the related snow layers showed a predominant organic composition (50%), suggesting a probable predominance of ash and other carbonaceous material [22].

CONCLUSIONS

Snow formaldehyde content has been monitored in Antarctica over a large area of the Ross Sea sector. The large number of analyzed samples (over 1800) allowed a reliable, even if preliminary, statistical investigation of the spatial and temporal distribution of this component in coastal and plateau areas of Northern Victoria Land.

The relatively low background values (few micrograms per liter) seem to be largely insensitive to changes in geographical position of the sampling station, particularly in relation to altitude and distance from the sea. This pattern suggests that HCHO is uniformly distributed in the gas phase or in the finest aerosol fraction over the sampled areas, indicating a prevalent *in situ* formation and/or fast atmospheric transport toward inland plateau regions.

In some coastal and semi-plateau stations, the background values are modulated by high HCHO deposition events, occurring over relatively large time periods, such as biomass burning episodes probably encouraged by climatic and environmental variations on a regional scale.

Temporal profiles give no evidence of any post-depositional effects able to change the original composition of snow deposition, at least in the observed time period. Indeed, unlike chloride and nitrate [25], no decrease in the uppermost layer is visible, even in stations characterized by low snow accumulation rates, such as Dome C (about $30\,kg\,m^{-2}\,yr^{-1}$). Therefore, HCHO could be used as a marker of the past oxidizing capacity of the troposphere and of the presence of carbon-cycle compounds.

Further studies are needed to clarify HCHO sources and its role in the atmospheric and snow chemistry in the Antarctic ice sheet.

References

[1] J. Slemr and W. Junkermann, *Atmos. Environ.*, **30**, 3667–3676 (1996).
[2] R. Holzinger, C. Warneke, A. Hansel, A. Jordan, W. Lindinger, D.H. Scharffe, G. Schade and P.J. Crutzen, *Geoph. Res. Lett.*, **26**, 1161–1164 (1999).
[3] J.G. Goode, R.J. Yokelson, D.E. Ward, R.A. Susott, R.E. Babbitt, M.A. Davies and W.M. Hao, *J. Geoph. Res.*, **105**, 22147–22166 (2000).
[4] Air Quality Guidelines for Europe, WHO European Series No. 23, WHO Copenhagen (1987).
[5] A.L. Sumner and P.B. Shepson, *Nature* **398**, 230–233 (1999).
[6] V. Wagner, R. von Glasow, H. Fisher and P.J. Crutzen, *J. Geoph. Res.*, **107**, 1–14 (2002).
[7] Y.-N. Lee, X. Zhou, L.I. Kleinman, L.J. Nunnermacker, S.R. Springston, P.H. Daum, L. Newman, W.G. Keigley, M.W. Holdren, C.W. Spicer, W. Young, B. Fu, D.D. Parrish, J. Holloway, J. Williams, J.M. Roberts, T.B. Ryerson and F.C. Fehsenfeld, *J. Geoph. Res.*, **103**, 22449–22462 (1998).
[8] K. Fuhrer, M. Hutterli and J.R. McConnell, In: E.W. Wolff and R.C. Bales (Eds.), *Processes of Chemical Exchange between the Atmosphere and Polar Snow*, NATO ASI Series I. Springer Verlag, Berlin (1996).
[9] K. Riedel, R. Weller and O. Schrems, *Phys. Chem. Chem. Phys.*, **1**, 5523–5527 (1999).
[10] R.W. Gillett, T.D. van Ommen, A.V. Jackson and G.P. Ayers, *J. Glaciol.*, **46**, 15–19 (2000).

[11] R. Röthlisberger, M. Bigler, M. Hutterly, S. Sommer, B. Stauffer, H.G. Junghans and D. Wagenbach, *Environ. Sci. Technol.*, **34**, 338–342 (2000).
[12] J. Tschumi and B. Stauffer, *J. Glaciol.*, **46**, 45–53 (2000).
[13] S. Dong and P.K. Dasgupta, *Environ. Sci. Technol.*, **21**, 581–588 (1987).
[14] O. Largiuni, R. Udisti, R. Traversi and G. Piccardi, *Int. J. Environ. Anal. Chem.* **82**, 97–112 (2002).
[15] R. Udisti, E. Barbolani, S. Becagli and G. Piccardi, *Terra Antartica Rep.*, **1**, 109–113 (1997).
[16] G. Piccardi, E. Barbolani, S. Bellandi, F. Casella and R. Udisti, *Terra Antartica*, **1**, 134–137 (1994).
[17] G. Piccardi, R. Udisti and F. Casella, *Intern. J. Environ. Anal. Chem.*, **55**, 219–234 (1994).
[18] R. Udisti, *Intern. J. Environ. Anal. Chem.*, **63**, 225–244 (1996).
[19] K. Fuhrer, A. Neftel, M. Anklin and V. Maggi, *Atmos. Environ.*, **27A**, 1873–1880 (1993).
[20] M.A. Hutterli and R. Röthlisberger, *Geophys. Res. Lett.* **26**, 1691–1694 (1999).
[21] S. Becagli, S. Benassai, E. Castellano, O. Largiuni, A. Migliori, R. Traversi, O. Flora and R. Udisti, *Intern. J. Environ. Anal. Chem.*, **84**, 523–536 (2004).
[22] V. Maggi, Personal communication (2000).
[23] V. Maggi and J.R. Petit, *Ann. Glac.*, **27**, 355–359 (1998).
[24] R. Udisti, S. Becagli, R. Traversi, S. Vermigli and G. Piccardi, *Ann. Glac.*, **27**, 391–397 (1998).
[25] R. Traversi, S. Becagli, E. Castellano, O. Largiuni and R. Udisti, In: M. Colacino and G. Giovanelli (Eds.), *Proceeding of the 8th Workshop on Italian Research on the Antaritic Atmosphere*, Vol 69. SIF Bologria (2000).